

Available online at www.sciencedirect.com

jmr&t
Journal of Materials Research and Technology
journal homepage: www.elsevier.com/locate/jmrt



Original Article

Cold-pressed fly ash geopolymers: effect of formulation on mechanical and morphological characteristics



Ong Shee-Ween ^{a,b}, Heah Cheng-Yong ^{a,c,*}, Liew Yun-Ming ^{a,b},
Mohd Mustafa Al Bakri Abdullah ^{a,b}, Ho Li Ngee ^{a,b},
Lynette Wei Ling Chan ^d, Ooi Wan-En ^{a,b}, Nur Ain Jaya ^{a,b},
Ng Yong-Sing ^{a,b}

^a Geopolymer and Green Technology, Centre of Excellence (CEGeoGTech), Universiti Malaysia Perlis (UniMAP), 01000 Perlis, Malaysia

^b Faculty of Chemical Engineering Technology, Universiti Malaysia Perlis (UniMAP), 01000 Perlis, Malaysia

^c Faculty of Mechanical Engineering Technology, Universiti Malaysia Perlis (UniMAP), 02600 Perlis, Malaysia

^d Ceramic Research Company Sdn Bhd (Guocera-Hong Leong Group), Lot 7110, 5 ½ Miles, Jalan Kapar, 42100 Klang, Selangor, Malaysia

ARTICLE INFO

Article history:

Received 20 May 2021

Accepted 20 September 2021

Available online 30 September 2021

Keywords:

Geopolymer

Cold press

Fly ash

Compressive strength

Flexural strength

ABSTRACT

This research uses low alkali activator content and cold pressing technique for fly ash-based geopolymers formation under room temperature condition. The geopolymers were prepared using four different parameters: fly ash/alkali activator ratio, sodium hydroxide concentration, sodium silicate/sodium hydroxide ratio and pressing force. The results indicated that the compressive strength (114.2 MPa) and flexural strength (29.9 MPa) of geopolymers maximised at a fly ash/alkali activator ratio of 5.5, a 14 M sodium hydroxide concentration, a sodium silicate/sodium hydroxide ratio of 1.5 and a pressing force of 5 tons (pressing stress of 100.0 MPa and 155.7 MPa for compressive and flexural samples, respectively). The degree of reaction (40.1%) enhanced the structure compactness with minimum porosity. The improved mechanical properties confirmed that a high strength pressed geopolymer could be formed at low alkali activator content without the aid of temperature.

© 2021 The Author(s). Published by Elsevier B.V. This is an open access article under the CC BY-NC-ND license (<http://creativecommons.org/licenses/by-nc-nd/4.0/>).

* Corresponding author.

E-mail address: cyheah@unimap.edu.my (H. Cheng-Yong).

<https://doi.org/10.1016/j.jmrt.2021.09.084>

2238-7854/© 2021 The Author(s). Published by Elsevier B.V. This is an open access article under the CC BY-NC-ND license (<http://creativecommons.org/licenses/by-nc-nd/4.0/>).

1. Introduction

The manufacturing process of Portland cement is an energy-intensive process since a high temperature is required to produce the clinker. Furthermore, the synthesis of cementitious concrete involves many carbon dioxide emissions due to the de-carbonation of the limestone. Depending on the clinker content, the carbon dioxide emission could be as high as 0.9 kg for every 1 kg of cement produced, amounting to around 5% of global human-made carbon dioxide emissions and contributing to global warming and the greenhouse effect [1]. In short, this phenomenon has a tremendous impact on both our environment and the area of sustainable development.

Given lower carbon dioxide emission involvement, geopolymers have received a great deal of attention among researchers. Geopolymer is an essential cementitious material that is primarily used in the construction field. The comparatively lower energy consumption in geopolymer production, compared to Portland cement, means geopolymers fulfil the widespread demand for eco-friendly construction material. Geopolymer is an inorganic binder composed of an amorphous and tri-dimensional network, resulting from the alkali activation of aluminosilicate monomers. Materials that are rich in silica and alumina are the primary requirement for classification as an aluminosilicate monomer [2]. In addition to dehydroxylated clays, such as metakaolin, various industrial by-products comprised of fly ash, slag and rice husk can be mixed with an alkali activator for dissolution and subsequent geopolymerisation. Hence, geopolymers are more favourable than Portland cement since a wide range of industrial waste products can be reused as aluminosilicate materials in manufacturing the geopolymers [3].

Conventionally, geopolymers is formed from normal casting method which have certain limitations in generating a highly compact geopolymer structure. This is because the casting method requires higher alkali activator content, leading to a highly porous microstructure. Thus, it is difficult to synthesise a geopolymer with a 28-day compressive strength of higher than 50 MPa at ambient temperatures [4–6]. Here, reducing the alkali activator content and using high pressure for the compaction of fresh geopolymer paste could solve the aforementioned problem. The use of a pressing method in the manufacturing of geopolymers remains comparatively rare, while it has been widely applied in ceramics production [7–9].

Several studies have reported that the fabrication of geopolymers via pressure compaction helps to remove a large proportion of the trapped air bubbles formed between the particles. The process significantly reduces the forming structure's porosity, accompanied by a dense micromorphology [10–12]. Alshaaer [13] largely succeeded in improving the mechanical properties (59 MPa) of a kaolinite-based geopolymer after pressing at 15 MPa, while a pressed geopolymer with a compressive strength of 65 MPa was achieved by Wang et al. [14]. However, the pressing method's low water content left a significant amount of metakaolinite, which remained intact during the geopolymerisation and moulding process, as indicated by the scanning electron microscopy (SEM) micrographs. Nonetheless, the various findings have demonstrated that the application of pressure has a significant impact on geopolymers in terms of compressive strength.

Meanwhile, Takeda et al. [15] achieved a higher degree of strength with a warm press method by applying high pressure and high temperature to the starting materials simultaneously. The resulting product had a maximum strength of 149 MPa after pressing with 200 MPa under a temperature of 130 °C for 1 h. However, this technique required a heat source to obtain the high strength geopolymer, and such a high manufacturing temperature will prove more challenging to handle in mass production processes. Furthermore, the warm press method is also limited as a production tool given the attendant high production costs and comparatively low productivity [16]. In a more recent work carried out by Prasphan et al. [10], the compressive strength of cold-pressed geopolymer was 27 MPa only after 7 days of curing. Nevertheless, while it was not as strong the hot-pressed geopolymer, room temperature curing in cold-pressed geopolymers is advantageous since it uses less energy throughout the entire manufacturing process. Therefore, reducing the energy consumption per product is feasible. Moreover, optimising the compositional mixing design of pressed geopolymers forms a comparably strong geopolymer at ambient temperatures.

Various studies [11,17,18] related to the effect of mix proportion and pressing force on the properties of pressed geopolymers have been carried out. Here, the preparation method

Table 1 – Chemical composition of fly ash.

Compound	Weight percentage (wt.%)
Silicon dioxide (SiO ₂)	36.1
Iron oxide (Fe ₂ O ₃)	19.1
Aluminium oxide (Al ₂ O ₃)	18.1
Calcium oxide (CaO)	16.2
Magnesium oxide (MgO)	3.8
Potassium dioxide (K ₂ O)	1.8
Sulphur trioxide (SO ₃)	1.5
Titanium dioxide (TiO ₂)	1.1
Sodium oxide (Na ₂ O)	1.0
Other oxides	1.3

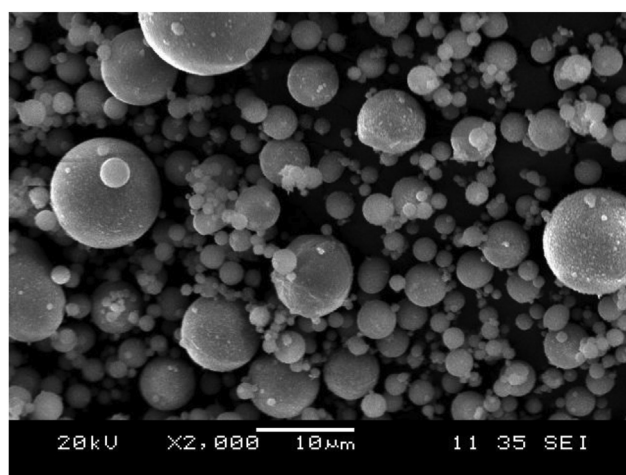


Fig. 1 – SEM micrograph of fly ash.

Table 2 – Mix proportions and pressing force of pressed geopolymer specimens.

Series	Design variables			
	S/L ratio ^a	NaOH concentration (M)	SS/NaOH ratio ^a	Pressing force (tons)
S/L ratio	4.5, 5.5, 6.5, 7.0	10	1.0	5
NaOH concentration	5.5	10, 12, 14, 16	1.0	5
SS/NaOH ratio	5.5	14	1.0, 1.5, 2.0, 2.5	5
Pressing force (tons)	5.5	14	2.0	3, 4, 5, 6

^a Mass/mass ratio.

utilised by Ranjbar et al. [17] was the hot-pressing method. At the same time, the study of Posi et al. [18] involved the use of fly ash and ordinary Portland cement as the source materials and the study of Wang et al. [11] used metakaolin and fly ash with epoxy as an additive. In contrast, the present study employs the cold-pressing method and utilises fly ash alone as the raw material. Meanwhile, the above studies were largely focused on the effect of formulation and pressing force on the compressive strength and microstructural changes in pressed geopolymers, while the flexural strength development and the degree of reaction were not discussed.

Further studies are thus required to highlight the impact of mix design and pressing force on the flexural strength of pressed geopolymers. The data related to flexural strength could potentially reveal the ability of pressed geopolymers to withstand bending force and widen the new application possibilities of pressed geopolymers in fields such as the tile industry. Furthermore, it is vital to maximise the use of raw materials in geopolymer production since this is the key factor in governing their engineering properties and microstructure. While the low alkali activator content used in the pressing method will likely limit the reactivity of the raw materials, the silicate and aluminate content available in geopolymerisation could be increased by optimising the mix design and pressing force.

This, therefore, brings the focus to the possibility of forming high strength geopolymers with low alkali activator content alongside pressure compaction without the aid of temperature. In the present study, fly ash and an alkali activator were mixed to form a dry mix, which was then pressed using a 5-ton pressure for 2 min before being cured at room temperature for two different periods (7 and 28 days). The optimisation of the mix proportion (fly ash/alkali activator ratio, sodium hydroxide concentration, sodium silicate/sodium hydroxide ratio) and the pressing force of the pressed geopolymer was subsequently evaluated. They were regarded

as the main determining factors in the properties of the end product. Overall, the present study highlights the influence of mix proportion and pressing force on the extent of the reaction and the physical and mechanical properties of geopolymers prepared via the cold-pressing method, while the possible reaction mechanism of pressed geopolymers is also discussed.

2. Experimental work

2.1. Materials

2.1.1. Fly ash

Fly ash procured from Manjung Coal-fired Power Plant, Perak was used as a starting material. The chemical composition of fly ash (Table 1) was determined by X-ray fluorescence (XRF) spectroscopy. The fly ash consisted of 36.1% SiO₂, 19.1% Fe₂O₃, 18.1% Al₂O₃ and 16.2% CaO. Therefore, it was class F fly ash as per ASTM C618-19. The SEM micrograph of fly ash as depicted in Fig. 1 indicated that the fly ash particles were spherical with a smooth surface texture. The spherical shape of fly ash increases its reactivity and thus facilitates geopolymerisation reaction.

2.1.2. Alkali activator

The use of sodium hydroxide (NaOH) in conjunction with sodium silicate (Na₂SiO₃) can speed up the geopolymerisation reaction and strengthen the final products. Thus, this study employed a mixture of NaOH and Na₂SiO₃ for the synthesis of pressed geopolymer. The NaOH pellets have 99% purity, while the Na₂SiO₃ solution consists of 60.5 wt.% of H₂O, 30.1 wt.% of SiO₂ and 9.4 wt.% of Na₂O. The NaOH solution was obtained by dissolving the caustic soda flakes with distilled water and allowed to equilibrate at room temperature for 24 h before use to ensure the complete dilution of the caustic soda flakes.

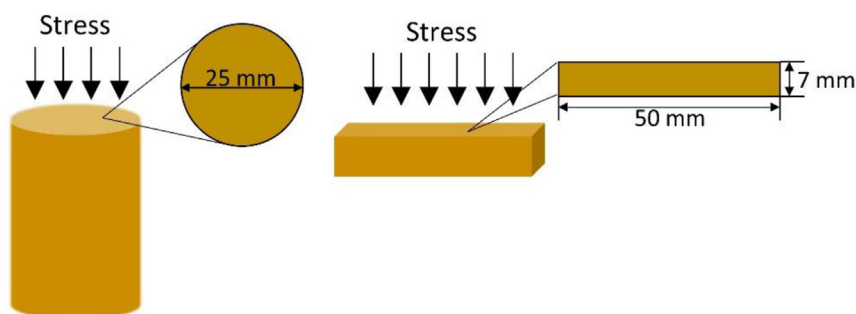


Fig. 2 – Plane of compression and flexural geopolymer samples that the pressing force is applied on.

Table 3 – Applied stress of compression and flexural samples at different pressing force.

Pressing force (ton)	Applied stress (MPa)	
	Compression sample	Flexural sample
3	60.0	93.4
4	80.0	124.6
5	100.0	155.7
6	120.0	186.9

2.2. Mixing, pressing and curing

The preparation of semi-dry and homogeneous mixture involved the addition of alkali activator to fly ash and hand-mixed for 5 min. The semi-dry mix was poured into a stainless-steel pressing mould, then manually pressed using a hydraulic press for 5 tons. In this study, two types of samples were fabricated, in which cylindrical sample ($\phi = 25 \text{ mm} \times 50 \text{ mm}$) was used for compression testing while cuboid sample ($50 \text{ mm} \times 5 \text{ mm} \times 7 \text{ mm}$) was used for flexural testing. After 2 min of compaction, the geopolymer samples were removed from the mould and wrapped with plastic film to avoid moisture loss. The samples were cured at room temperature for 7 and 28 days before the day of testing.

For adequate data, geopolymers with various mix proportions were made as shown in Table 2 in which four series of samples were prepared to investigate the impact of fly ash/alkali activator (S/L) ratio (4.5, 5.5, 6.5 and 7.0), sodium hydroxide concentration (10, 12, 14 and 16 M), sodium silicate/sodium hydroxide (SS/NaOH) ratio (1.0, 1.5, 2.0 and 2.5) and pressing force (3, 4, 5 and 6 tons) on the properties of pressed geopolymer. The optimised mix formulation from previous series was carried forward and employed in the following series.

Based on Table 2, the pressing force was set in the range of 3–6 tons during the cold-pressing process. However, the stress induced on the cylindrical and cuboid samples was different attributed to the varied cross-sectional area of the plane which the pressing force applied on (Fig. 2). Table 3 enlists the induced stress of compression and flexural samples according to the pressing force applied. In order to standardized the parameter used, pressing force was reported as one of the factor in this study instead of stress.

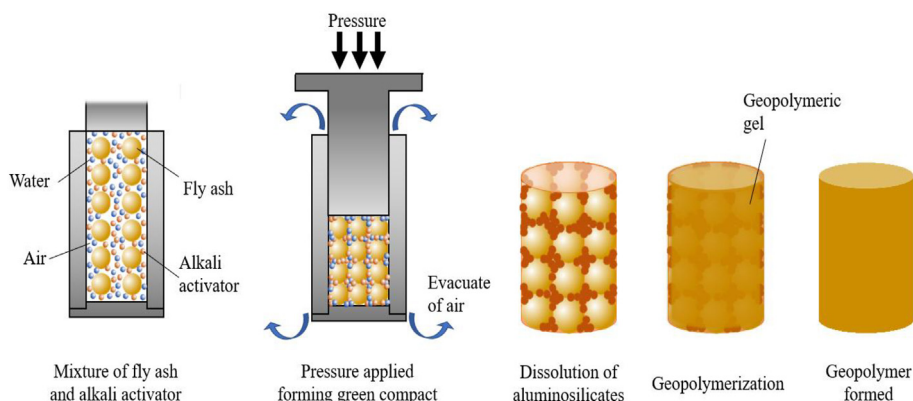


Fig. 3 – Proposed mechanism of geopolymer fabricated via the pressing method.

2.3. Testing method and analysis

The physical analysis of the pressed geopolymer was evaluated using the cylindrical compressive strength specimens that aged for 7 and 28 days. The bulk density of synthesized pressed geopolymers was conducted according to ASTM C39.

The porosity measurement of pressed geopolymer was performed by emerging the samples in water for 24 h and dried with lint-free cloth to obtain W_s . The samples were then fully submerged in water and weighed as W_i , while the weight of oven-dried samples was recorded as W_d . The percentage of porosity of the samples was calculated using Equation (2).

$$\text{Percentage of porosity} = \frac{(W_s - W_d)}{(W_s - W_i)} \times 100\% \quad (2)$$

where W_s is the saturated weight, W_d is the oven-dry weight and W_i is the immersed weight of the specimen.

The water absorption measurement of pressed geopolymers was carried out according to ASTM C140. The percentage of water absorption was calculated using Equation (3).

$$\text{Percentage of water absorbed} = \frac{(W_s - W_d)}{W_d} \times 100\% \quad (3)$$

The compressive strength of specimens was examined in accordance with ASTM C39 using Instron Machine Series 5569 Mechanical Tester with a constant loading rate of 1 mm/min. A minimum of three cylindrical specimens was tested for every mixture. The average values of 7-day and 28-day compressive strength were then calculated.

Besides, the flexural strength of each cuboid specimen was obtained using a standard three-point-bending test at a loading rate of 0.5 mm/min. The flexural strength was determined using Equation (4). The stiffness of geopolymer was calculated through the best linear regression of stress–strain curve of specimens.

$$\text{Flexural strength} = \frac{3P_m S}{2BW^2} \quad (4)$$

where P_m is the maximum load, S is the span length of specimen, B is the width of specimen and W is the thickness of specimen.

The degree of reaction of pressed geopolymer was determined by selective chemical attack using hydrochloric acid (HCl) and sodium carbonate (Na_2CO_3) solutions. The use of HCl

Table 4 – Physical properties of pressed geopolymer with different S/L ratio.

S/L ratio	Density (kg/m ³)		Porosity (%)		Water absorption (%)	
	7 days	28 days	7 days	28 days	7 days	28 days
4.5	2125 ± 4.7	2131 ± 6.5	16.1 ± 0.2	13.7 ± 0.5	9.8 ± 0.1	8.5 ± 0.3
5.5	2191 ± 5.1	2179 ± 1.7	11.1 ± 0.1	9.2 ± 0.5	6.6 ± 0.1	5.4 ± 0.3
6.5	2158 ± 6.9	2150 ± 4.6	13.0 ± 0.4	9.6 ± 0.4	6.6 ± 0.3	5.7 ± 0.3
7.0	2144 ± 4.8	2139 ± 2.3	12.9 ± 0.4	10.8 ± 0.0	7.8 ± 0.2	6.6 ± 0.0

Remark: ± represents the standard deviation.

and Na₂CO₃ solutions separated out the geopolymeric gel and unreacted fly ash, in which the solutions dissolve the products of alkaline activation leaving unreacted fly ash as insoluble residue. The degree of reaction of geopolymer was determined by measuring the insoluble residue in the mixture. 3 g of geopolymer powder was dissolved in 30 ml of 2 M HCl. The mixture was placed in water bath at 60 °C and stirred at a constant speed for 20 min. The mixture was filtered through filter paper while the residue was washed with warm water at least 3 times to remove HCl. The insoluble residue was oven-dried at 80 °C for 2 h. Afterward, the residue was dissolved in 30 ml of 3% Na₂CO₃. The mixture was placed in 60 °C water bath and stirred continuously for 20 min. The mixture was filtered while the residue was washed with warm water rapidly before oven drying. The weight of the dried insoluble residue (unreacted fly ash) was measured by electronic balance. The degree of reaction of pressed geopolymer was calculated using Equation (5) [19,20]. The degree of reaction of geopolymer samples are subtracted with the degree of reaction of source material. The degree of reaction calculated is the corrected degree of reaction of geopolymer.

$$\text{Degree of reaction} = \frac{W_{\text{sample}} - W_{\text{residue}}}{W_{\text{sample}}} \times 100\% \quad (5)$$

where W_{sample} is the weight of geopolymer sample in powder form (g), while W_{residue} is the weight of oven dried residue (g).

On the basis of results acquired in this study, statistical analysis with the one-way ANOVA study was performed at the confidence level of 95%. The *F*-values in ANOVA analysis were used to determine the statistical significance of design

variables (that are, S/L ratio, NaOH concentration, SS/NaOH ratio and pressing force) on the properties of pressed geopolymer with 5% significance level.

Using scanning electron microscopy (SEM) model JSM-6460LA, the morphology of 28-day pressed geopolymer was revealed with 25 kV electron beam energy and 10 mm working distance. In order to identify the mineral phases of geopolymers, X-ray diffraction (XRD) analysis was performed using Shimadzu x-ray diffractometer XRD-6000. The XRD patterns were measured from 10 to 80° 2θ with a scanning rate of 0.1 step/s.

Fourier transform infrared (FTIR) data of geopolymers were collected using the Perkin Elmer Fourier Transform Infrared Spectroscopy (FTIR) RXI spectrometer, equipped with a diamond crystal. The samples were scanned over a range of 500 cm⁻¹–4000 cm⁻¹ using 4 cm⁻¹ resolutions.

3. Results and discussion

3.1. Proposed mechanism of the pressing method

Fig. 3 presents a schematic of the proposed mechanism of pressed geopolymers. By utilising the pressing method, precursors were densified and compacted via an applied force in a confined space. During the initial compaction, the removal of the trapped air in conjunction with the internal motion of the particles was incidental to the consolidation via a unidirectional pressing force [21]. Hence, the particles were rearranged, which increased the inter-particle contact and

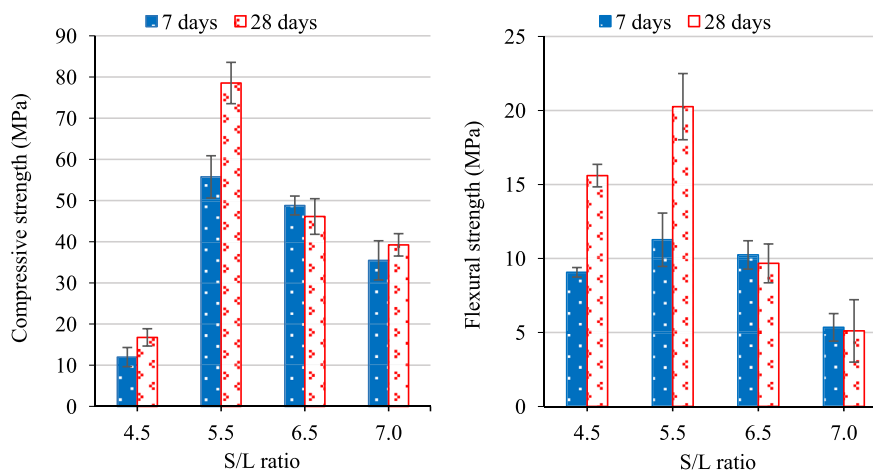


Fig. 4 – 7-day and 28-day compressive and flexural strengths of pressed geopolymer with different S/L ratio.

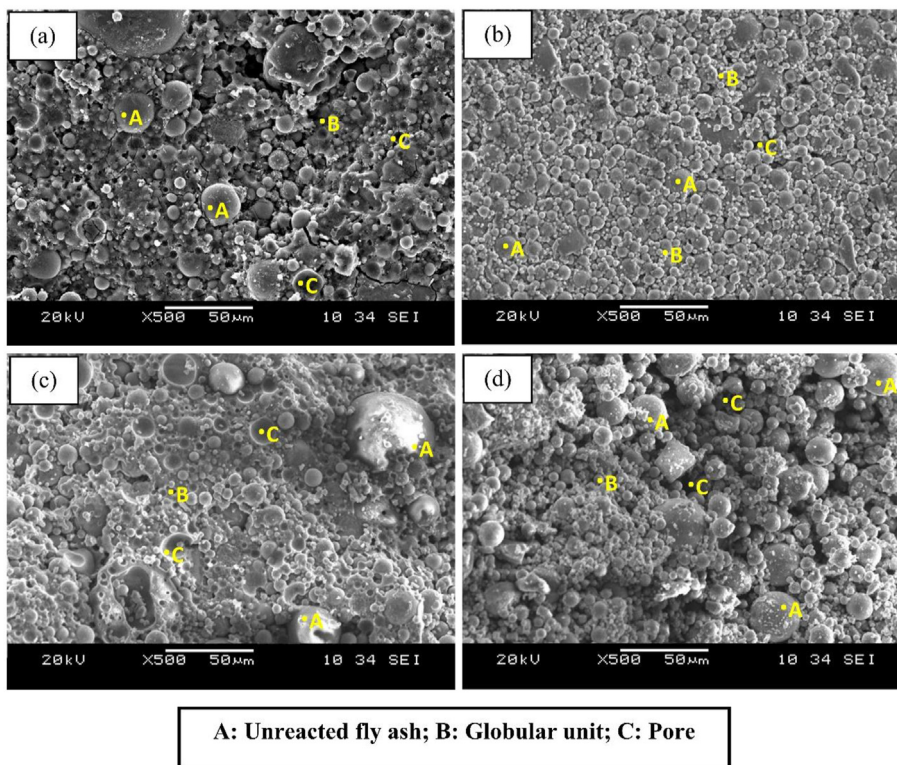


Fig. 5 – SEM micrographs of pressed geopolymers with S/L ratios of (a) 4.5; (b) 5.5; (c) 6.5; and (d) 7.0 after ageing for 28 days.

contributed to a well-packed mixture. This phenomenon led to a loss in pressure attributed to the removal of air that trapped within the spherical particles. When the pressure was increased to the initial condition, the particle rearrangement occurred, which further improved the mixture compactness and structure density.

The well-compacted mixture caused the geopolymerisation reaction to occur on the adjacent surface between the fly ash particles and the alkali activator. Dissolution occurred via alkaline hydrolysis at the surface of these fly ash particles, forming dissolved Si^{4+} and Al^{3+} ions. Meanwhile, in the presence of the alkali activator, the ions combined to form tetrahedral and silicate monomers, which subsequently underwent polymerisation to form a geopolymer matrix. As the matrix grew bigger, the system continued to undergo rearrangement, resulting in tri-dimensional aluminosilicate geopolymer networks. These networks increased according to the curing time, and it was thus deemed that the geopolymerisation was inherently time-dependent.

3.2. Effect of S/L ratio

Table 4 shows the bulk density, percentage of porosity and water absorption of the pressed geopolymers prepared using various S/L ratios. The attendant analyses were carried out at a constant NaOH concentration and SS/NaOH ratio of 10 M and 1.0, respectively. Here, the pressed geopolymer achieved the highest bulk density and the lowest percentage of porosity and water absorption when the S/L ratio was 5.5.

Applying a pressing force can improve the compactness of fly ash particles and thus reduce the alkali activator requirement. However, an inadequate alkali activator amount will give rise to the poor development of the geopolymer matrix and result in the formation of pores at the spaces between the unreacted fly ash particles. This behaviour was observed in the pressed geopolymers with S/L ratios of 6.5 and 7.0, with the specimens exhibiting a slight increment in porosity and water absorption.

Table 5 – Physical properties of pressed geopolymer prepared by various NaOH concentrations.

NaOH molarity (M)	Density (kg/m^3)		Porosity (%)		Water absorption (%)	
	7 days	28 days	7 days	28 days	7 days	28 days
10	2191 ± 5.1	2179 ± 1.7	11.1 ± 0.1	9.2 ± 0.5	6.6 ± 0.1	5.4 ± 0.3
12	2196 ± 2.9	2194 ± 4.7	10.3 ± 0.4	8.6 ± 0.5	6.1 ± 0.3	5.0 ± 0.3
14	2208 ± 4.7	2202 ± 1.7	9.7 ± 0.4	8.1 ± 0.0	5.8 ± 0.4	4.7 ± 0.1
16	2198 ± 1.6	2193 ± 3.1	9.6 ± 0.1	8.9 ± 0.3	5.7 ± 0.3	5.2 ± 0.2

Remark: ± represents the standard deviation.

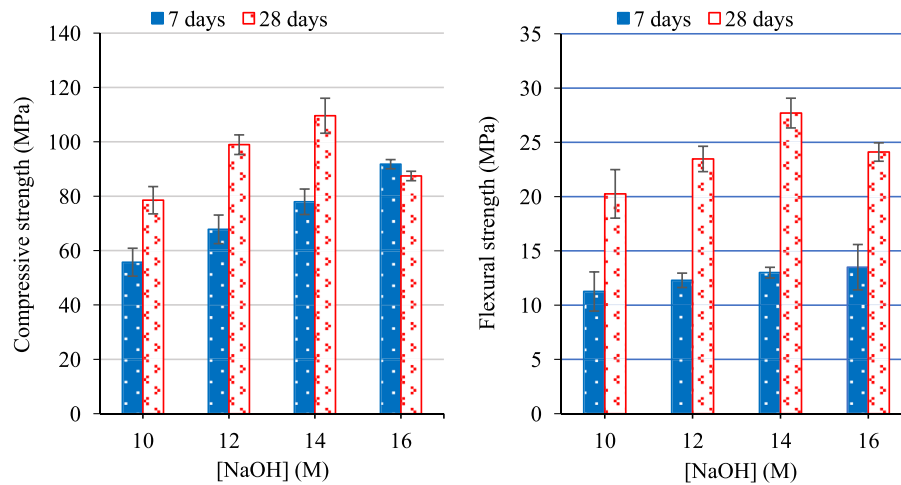
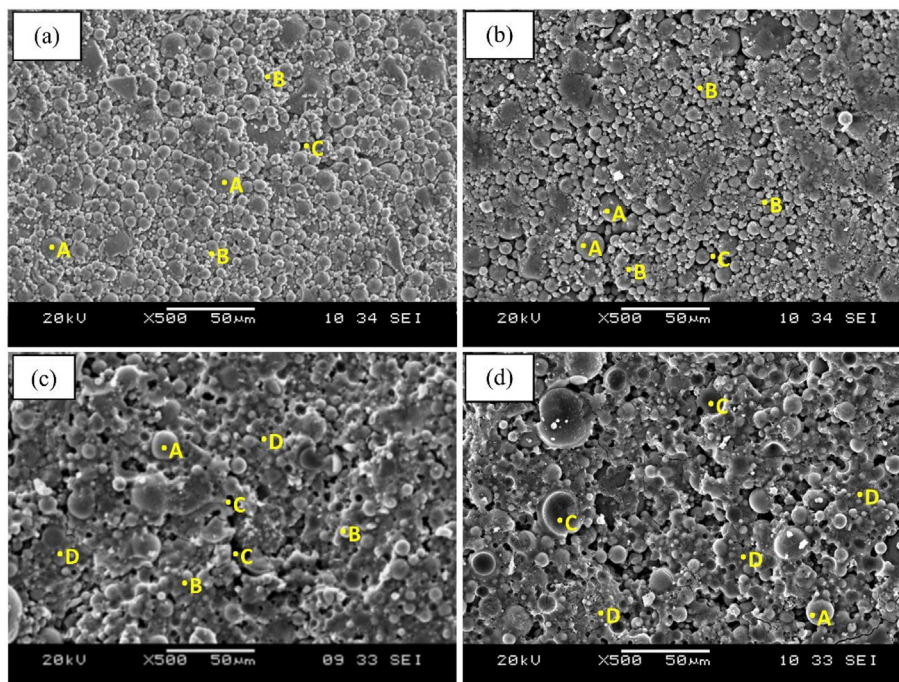


Fig. 6 – 7-day and 28-day compressive and flexural strengths of pressed geopolymer with different NaOH concentrations.

Overall, the S/L ratio had a significant effect on the development of the mechanical strength of the pressed geopolymers (Fig. 4), with that prepared using an S/L ratio of 5.5 exhibiting a maximum 28-day compressive and flexural strengths of 78.5 and 20.3 MPa, respectively. It appears that the S/L ratio of 5.5 had the optimum alkali activator content to drive faster silica dissolution and assist in developing an optimum geopolymerisation while not causing an overflow of the geopolymer mixture when pressure was exerted on the steel mould.

According to previous studies [22–24], a lower S/L ratio within the 0.71–3.0 range is commonly used in casted geopolymers. Nevertheless, this is generally not the case for geopolymers fabricated via the pressing method. The excessive activating solution forms a watery mix, which leads to a problem in the pressing process, a phenomenon supported by Posi et al. [18]. Notwithstanding, Ranjbar et al. [17] reported different findings, ascertaining that a hot-pressed geopolymer with an S/L ratio of 2.86 exhibited the best mechanical performance. That was to say, geopolymers produced via the hot-



A: Unreacted fly ash; B: Globular unit; C: Pore; D: Geopolymer gel

Fig. 7 – SEM micrographs of pressed geopolymers after 28 days with NaOH concentrations of (a) 10 M; (b) 12 M; (c) 14 M; and (d) 16 M.

Table 6 – Physical properties of pressed geopolymer with different SS/NaOH ratio.

SS/NaOH ratio	Density (kg/m ³)		Porosity (%)		Water absorption (%)	
	7 days	28 days	7 days	28 days	7 days	28 days
1.0	2208 ± 4.7	2202 ± 1.7	9.7 ± 0.4	8.1 ± 0.0	5.8 ± 0.4	4.7 ± 0.0
1.5	2222 ± 3.2	2206 ± 4.7	7.8 ± 0.2	8.0 ± 0.0	4.6 ± 0.2	4.6 ± 0.0
2.0	2231 ± 6.4	2227 ± 5.3	7.5 ± 0.5	7.0 ± 0.3	4.4 ± 0.8	4.1 ± 0.1
2.5	2224 ± 2.7	2220 ± 2.9	8.9 ± 0.3	8.1 ± 0.3	5.3 ± 0.2	4.7 ± 0.1

Remark: ± represents the standard deviation.

pressing method require a relatively higher alkali activator content than those produced via the cold-pressing method because of the moisture loss when hot pressure is applied to the geopolymer mixture.

Moreover, the 28-day pressed geopolymers exhibited a greater degree of strength development, particularly those with an S/L ratio of 5.5, which exhibited an approximate 41% increment than the 7-day compressive strength. The effect of the S/L ratio was clearer in the later stages of the pressed geopolymer. However, the pressed geopolymers with a S/L ratio of higher than 5.5 exhibited a minimal strength increment due to the insufficient alkali activator content in conjunction with the moisture loss that obstructed the continual dissolution and condensation process.

The fly ash appeared spherical pearl-like particles (Fig. 1) and changed after geopolymerisation (Fig. 5). The pressed geopolymer formed a large number of globular units of geopolymeric gel with several unreacted fly ash particles. It was well known that the microstructure development of geopolymers begins with the precipitation of globular units of geopolymeric gel on the surface of fly ash particles. As the reaction continues, the globular units of geopolymeric gel bond closely and densify the geopolymer matrix. Instead of the formation of globular units, the surface of geopolymer covered by a smooth geopolymeric gel and reduced the number of unreacted fly ash. Hence, the reactivity of fly ash can be determined according to the amount of globular units formed. Due to the low alkali activator content used in the pressing method, a limited geopolymer matrix was formed,

but the compactness of microstructure enhanced with the exertion of pressing force. This reduced the pore formation in the pressed geopolymers compared to that observed in casted geopolymers. In general, the pressed geopolymers presented a distinct morphology from geopolymers prepared via the casting method.

The geopolymer with the S/L ratio of 4.5 had a morphology with a significant amount of pores, which corresponded to the difficulty in the pressing process for the geopolymer mix. The alkali activator was crucial in facilitating the dissolution of the raw materials but the surplus liquid content resulted in the geopolymer mixture overflowing during the compaction process. Despite this, the liquid content in the geopolymer with an S/L ratio of 4.5 remained the highest among all the geopolymers. This reduced the geopolymer's green strength, which could be a dominant issue since it would likely affect the resultant geopolymer's strength development.

As Fig. 5b shows, there was a clear improvement in the compactness of the geopolymers when utilising the S/L ratio of 5.5. The geopolymer with this S/L ratio presented a dense microstructure comprised of numerous well-compacted globular units, which effectively reduced the matrix's porosity (Table 4). This finding was corroborated by Wang et al. [11], who declared that a higher S/L ratio could bring down the porosity value of geopolymers. Meanwhile, according to Astutiningsih et al. [25], the reactivity of aluminosilicates is related to the number of globular units appearing in the geopolymer matrix. Hence, at an S/L ratio of 5.5, there is an adequate amount of alkali activator content to ensure

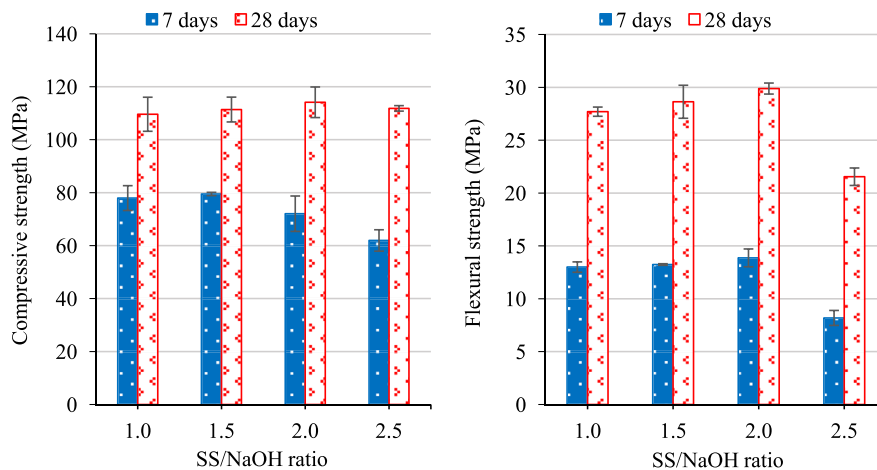


Fig. 8 – The 7-day and 28-day compressive and flexural strengths of pressed geopolymer with different SS/NaOH ratios.

pressure compaction without compromising the reactivity of fly ash. With the aid of pressure, a strong structural bonding can be attained with an optimal S/L ratio.

On the other hand, as Fig. 5c and d show, there were many heterogeneous unreacted spherical fly ash particles. The limited alkali activator content slowed down the dissolution rate of the fly ash particles and interfered with the geopolymerisation reaction, which increased the porosity of the geopolymer matrix (Table 4).

3.3. Effect of NaOH concentration

As shown in Table 5, the increase in NaOH concentration improved the bulk density and reduced the porosity and water absorption of the pressed geopolymers. This was undoubtedly the consequence of a high NaOH concentration that provided a sufficiently high pH environment to accelerate the dissolution of the fly ash particles. These aspects facilitated a high degree of geopolymerisation and contributed to the formation of a less permeable and less porous structure. Both the porosity and water absorption values, which were in line with each other, corroborated this.

The importance of NaOH concentration on the strength of geopolymers is unquestionable. The key role of the alkali activator in a geopolymer system is to enable the internal Si^{4+} and Al^{3+} components to leach out from the aluminosilicate source. Meanwhile, the degree of dissolution of the aluminosilicate source directly impacts the formation of a rigid geopolymer framework, which depends on the concentration of the NaOH solution.

As Fig. 6 shows, the 7-day strength of the pressed geopolymers increased with the increase in NaOH concentration from 10 to 16 M. The highest 28-day compressive strength of 109.6 MPa was obtained for the geopolymer fabricated using a concentration of 14 M, which indicated an improvement of 40.6% from 7 to 28 days. The maximum flexural strength achieved was 27.7 MPa, which exhibited an approximate 113.1% flexural strength gain after 28 days. The increasing NaOH concentration yielded a higher degree of polycondensation and an improved inter-particle bonding strength of the geopolymers. In contrast, the low alkaline medium provided an insufficient amount of OH^- ions to break down the glassy chain of the fly ash and thus reduced the efficiency of the dissolution of Si^{4+} and Al^{3+} ions from the ash. This tended to weaken the structure and the properties of the synthesised geopolymers. As a workaround, the mechanical development of the geopolymer was highly dependent on the degree of dissolution of the raw materials, which was governed by the NaOH concentration. Notably, the compressive strength achieved in this study was only slightly lower than that of the hot-pressed geopolymer (133 MPa) acquired by Ranjbar et al. [17]. The strength of the hot-pressed geopolymer was due to the assistance of temperature (heating temperature of 350 °C and heating duration of 20 min) alongside the exertion of pressure, which led to a rapid geopolymerisation reaction.

The 28-day strengths levelled off when the NaOH concentration was higher than optimal (16 M). This condition was largely associated with the excess OH^- ion concentration due to the high NaOH concentration, which led to the formation of

geopolymeric matrix precipitation at the early stages and thus retarded the kinetics of the reaction between the solid and fluid contents at the later stages. It can be said that the effect of ageing was more visible in the geopolymers with a moderate NaOH concentration (12–14 M), an observation that is supported by the findings of Nazari and Sanjayan [26]. In order to improve the economic feasibility, a suggestion has been made for the utilization of a moderate concentration of NaOH with a longer ageing time. In spite of the decreased compressive strength (87.5 MPa) obtained using 16 M NaOH, this was still higher than the values obtained by Livi et al. [27], who achieved an optimal compressive strength of 21.4 MPa, despite the geopolymers being cured at 85 °C for 22 h.

Overall, the NaOH concentration utilised to activate the reaction of pressed geopolymer was comparatively higher than that required for geopolymers manufactured via conventional casting methods. This was attributed to the high NaOH concentration, which reduced the water content, enabled the formation of a viscous solution and consequently increased the viscosity of the geopolymer mixture. It is potentially advantageous to strengthen the pressed geopolymer structure since the overflow of the geopolymer mixture can be avoided during the compaction process.

Fig. 7 demonstrates the microstructures of the pressed geopolymers with different NaOH concentrations after 28 days. Since the reaction of a pressed geopolymer can be regarded as a system with relatively low alkali activator content, it is reasonable to suppose that a certain amount of fly ash particles will remain inert after the chemical reaction. However, incremental NaOH concentrations reduced the amount of inert fly ash. The geopolymer matrix development was more distinctive.

The geopolymers prepared with 10 and 12 M of NaOH solution presented a substantial amount of remnant fly ash particles with the limited formation of a geopolymer matrix. This could be attributed to the low alkaline medium provoking a weak chemical reaction and restricting the generation of a sodium aluminosilicate matrix.

The microstructures of the pressed geopolymers using 14 and 16 M of NaOH solution were largely similar, with the surface of the unreacted fly ash covered by a geopolymer matrix. Here, the matrix filled in the pores, which densified the geopolymer structure and consequently improved terms of strength (Fig. 7). The difference here was that the geopolymer with the 14-M NaOH solution had a low pore formation compared to that with the 16-M NaOH solution. A relatively more intervening geopolymer matrix in the geopolymer activated with the 14-M NaOH solution implied a higher density of Si–O–Si bond formation, which prone to a more compact microstructure and better strength properties. This was corroborated by Wang et al. [14]. They confirmed that the optimum NaOH concentration could facilitate the decomposition of the aluminosilicate source and promote a rigid framework structure synthesis.

3.4. Effect of SS/NaOH ratio

The physical properties of the pressed geopolymers with various SS/NaOH ratios are presented in Table 6. By increasing the SS/NaOH ratio, the porosity and water absorption of the

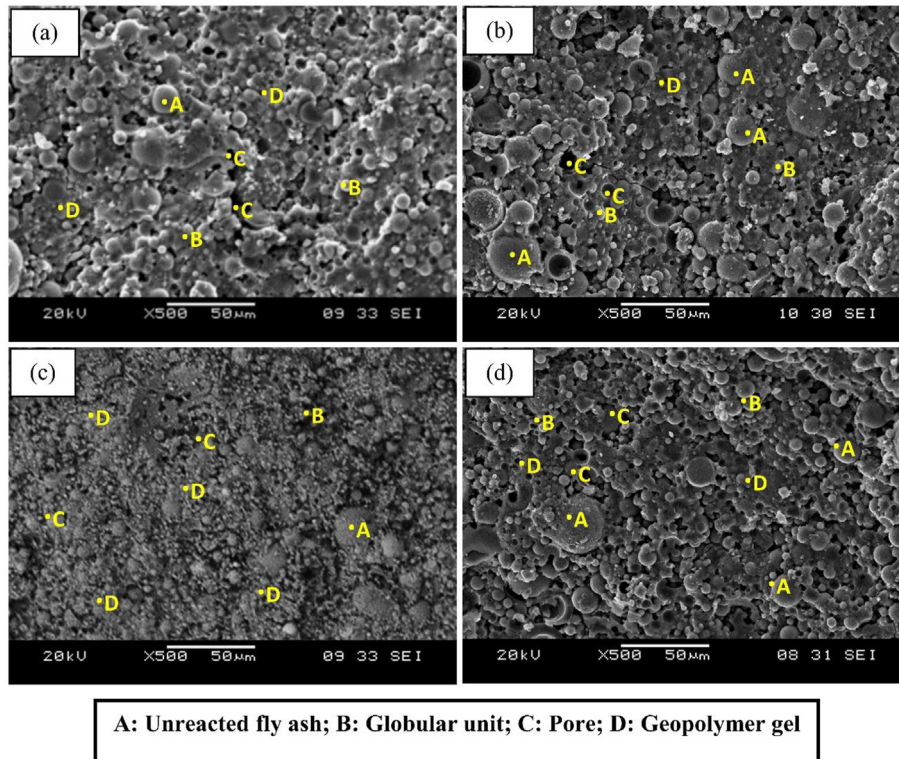


Fig. 9 – SEM micrographs of pressed geopolymers after 28 days with SS/NaOH ratios of (a) 1.0; (b) 1.5; (c) 2.0; and (d) 2.5.

pressed geopolymers were reduced, while a slight increment in bulk density was observed with the increase in SS/NaOH ratio. This was because the increasing sodium silicate content facilitated the occurrence of the geopolymerisation process, while the increase in bulk density was also attributed to the higher density of sodium silicate in comparison to sodium hydroxide solution. As previously ascertained by Posi et al. [28], the impact of the SS/NaOH ratio on the density of the geopolymers was insignificant.

Fig. 8 shows the strength development of the pressed geopolymers with various SS/NaOH ratios. In general, the increase in SS/NaOH ratio resulted in an improvement to the strength behaviour of the pressed geopolymers after 7 and 28 days, which was ascribed to the strengthening effect of the silica gel in the presence of the sodium silicate. The strength trend of the pressed geopolymers was in line with the corresponding bulk density results (Table 6).

Although sodium silicate played an important role in enhancing the geopolymerisation reaction, it must be considered that there should be an optimum SS/NaOH ratio for the geopolymer mixture. As seen, the 28-day compressive strength curve of the pressed geopolymers dipped at a SS/NaOH ratio of 2.5, which was in concert with the findings obtained by Hadi et al. [29]. The surplus sodium silicate content seemed to yield to the congestion of free Si^{4+} and Na^+ ions in the geopolymer matrix. This subsequently interfered with the geopolymerisation reaction and negatively influenced the mechanical performance of geopolymers. In addition, the high sodium silicate content increased the difficulty in compacting the geopolymer mixture, which was

attributed to the high stiffness of the mixtures, especially those with a comparatively high S/L ratio.

In the current study, the best performance geopolymer was obtained with a SS/NaOH ratio of 2.0, while the lowest strength was achieved at a SS/NaOH ratio of 1.0. These ratios were identical to those of the fly-ash-based geopolymers obtained by Hadi et al. [29]. Meanwhile, a lower SS/NaOH ratio (1.5) was reported by Esparham [30] in maximising the compressive strength of a metakaolin-based geopolymer. Based on the findings of Koushkbaghi et al. [31], the optimum SS/NaOH ratio could be different depending on the type of base material. The spherical morphology of fly ash reduces the particles' surface to volume ratio and lowers the water demands. Thus, a higher SS/NaOH ratio could be adopted in a fly-ash-based geopolymer mixture since the high sodium silicate content does not significantly affect the mix workability than a metakaolin mixture.

This notwithstanding, the 28-day compressive strength of the pressed geopolymers fell within the range of 109.6–114.1 MPa. The SS/NaOH ratio may have led to a limited variation in the compressive strength of the pressed geopolymers, especially after 28 days. From a cost-effective point of view, the use of sodium hydroxide is more desirable than sodium silicate. Although the maximum 28-day compressive strength was achieved with the pressed geopolymer prepared with a higher SS/NaOH ratio (2.5), the geopolymer mixtures with a lower SS/NaOH ratio (<2.0) were still acceptable since they satisfied the mechanical property requirements (>11.7 MPa) of construction materials, as specified in ASTM C90 and ASTM C39.

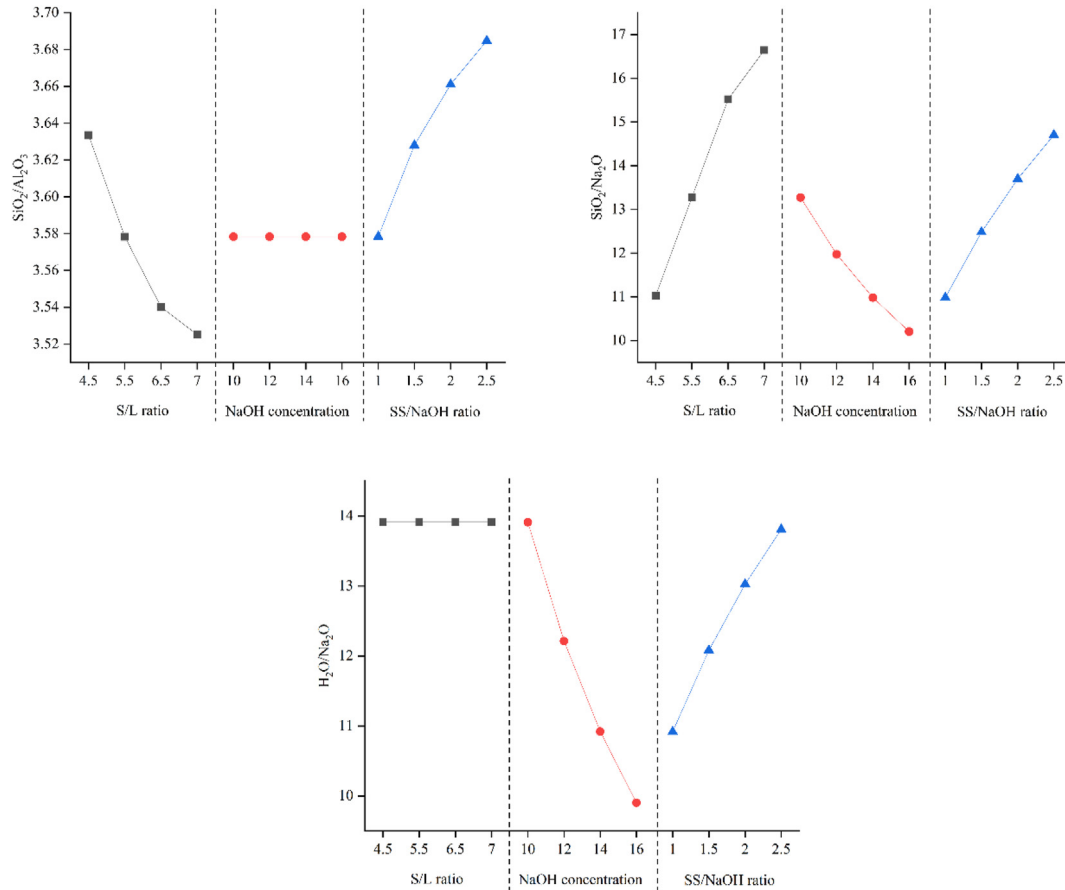


Fig. 10 – Oxide molar ratios of $\text{SiO}_2/\text{Al}_2\text{O}_3$, $\text{SiO}_2/\text{Na}_2\text{O}$ and $\text{H}_2\text{O}/\text{Na}_2\text{O}$ at different S/L ratio, NaOH concentration and SS/NaOH ratio.

Fig. 9 displays the microstructures of the pressed geopolymers with various SS/NaOH ratios. The microstructure of the pressed geopolymer with a SS/NaOH ratio of 1.0 indicated a greater number of pores and unreacted fly ash particles. Contrariwise, the geopolymer with a SS/NaOH ratio of 2.0 exhibited lower porosity and a more compact geopolymer gel structure, which further verified that a higher sodium silicate content is advantageous to the formation of geopolymers. This observation was corroborated by Haddad and Alshbuol [32], where the increase in SS/NaOH ratio gave rise to the formation of a more polymerised structure with fewer pores.

However, a higher quantity of partially reacted and unreacted particles were presented when the SS/NaOH ratio was higher than 2.0. This could be explained by the inadequate amount of sodium hydroxide, reducing the dissolubility

of the fly ash particles and causing them to become embedded in the geopolymer matrix. As stated by Almalkawi et al. [33], soluble silicate is crucial to ensure the appropriate polycondensation of geopolymers, provided an adequate amount of Si^{4+} and Al^{3+} ions are dissolved from the aluminosilicate materials. In short, for the effective dissolution of fly ash, a sufficient NaOH solution is vital.

3.5. Effect of initial oxide molar ratios

As shown in Fig. 10, the initial oxide molar ratios were determined according to the source materials and the alkali solution. By setting the NaOH molarity and SS/NaOH ratio at a constant value, the increase in S/L ratio corresponded to mixes with a decrease in $\text{SiO}_2/\text{Al}_2\text{O}_3$ and an increase in $\text{SiO}_2/$

Table 7 – Physical properties of pressed geopolymer with different pressing force.

Pressing force (t)	Density (kg/m^3)		Porosity (%)		Water absorption (%)	
	7 days	28 days	7 days	28 days	7 days	28 days
3	2182 ± 8.0	2184 ± 4.7	10.0 ± 0.1	8.0 ± 0.6	5.8 ± 0.0	4.8 ± 0.3
4	2188 ± 2.3	2181 ± 7.1	9.7 ± 0.0	8.2 ± 0.3	5.7 ± 0.0	4.8 ± 0.2
5	2231 ± 6.4	2227 ± 5.3	7.5 ± 0.5	7.0 ± 0.3	4.4 ± 0.3	4.1 ± 0.2
6	2212 ± 0.4	2201 ± 2.1	8.5 ± 0.1	7.5 ± 0.2	5.1 ± 0.1	4.3 ± 0.0

Remark: \pm represents the standard deviation.

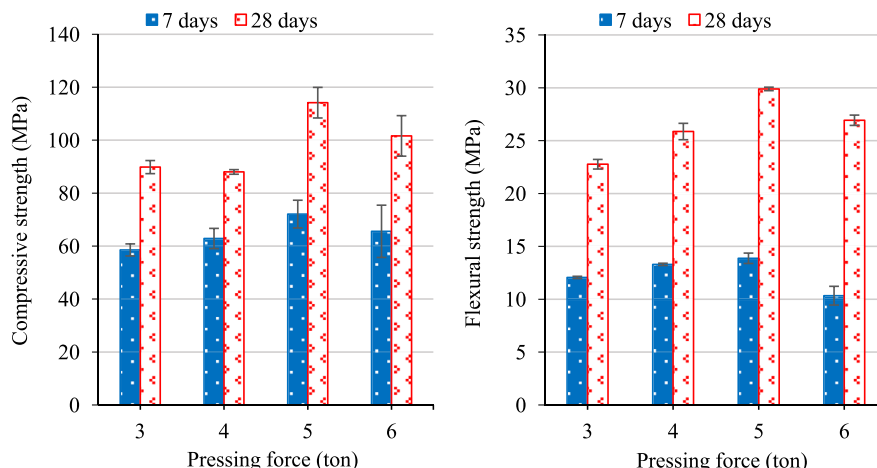


Fig. 11 – The 7-day and 28-day compressive and flexural strengths of pressed geopolymer with different pressing force.

Na₂O. At the same time, the H₂O/Na₂O remained unchanged. A similar situation occurred when increasing the SS/NaOH ratio with a constant S/L ratio and NaOH molarity, with the SiO₂/Al₂O₃, SiO₂/Na₂O and H₂O/Na₂O increasing. In contrast, an increase in NaOH concentration reduced the SiO₂/Na₂O and H₂O/Na₂O, while the SiO₂/Al₂O₃ remained the same. Based on the present study, the optimal SiO₂/Al₂O₃, SiO₂/Na₂O and H₂O/Na₂O initial molar ratios for maximising the compressive strength are 3.7, 13.7 and 13.0, respectively. Regardless of the increase in S/L ratio, NaOH concentration or SS/NaOH ratio, the optimal performance of pressed geopolymers is achievable at intermediate ratios. This suggests that the use of a high initial oxide molar ratio is not required to enhance the mechanical properties of end products.

The mechanical performance of the geopolymers related to the function of the SiO₂/Al₂O₃ ratio. The high SiO₂/Al₂O₃ ratio promoted strength enhancement as the formation of Si–O–Si bonds was more likely to occur than Si–O–Al and Al–O–Al bonds, which are weaker [34]. This statement was rationalized

by Juengsuwattananon et al. [35], who found that initial SiO₂/Al₂O₃ molar ratios of around 3.5–4.5 resulted in high compressive strength and durability. Further increasing the SiO₂/Al₂O₃ ratio degraded the strength of the pressed geopolymers due to the inhibition of the geopolymerisation through Al–Si phase precipitation. In other words, the surplus silicate content resulted in a lack of water evaporation and structure formation, which diminished the strength of the geopolymers.

Meanwhile, the SiO₂/Na₂O ratio was one of the influential parameters that affected the mechanical properties of the geopolymers. The Na₂O content in the alkali activator played a significant role in breaking down the glassy chain at the surface of the source materials. The Si and Al ions dissociated from the source materials prone to the formation of oligomeric silicate and aluminate species. After that, a condensation reaction took place between the oligomeric silicates and the Al(OH)₄⁻, causing the generation of networks of different types of structure. The Na₂O thus balanced out the charge of

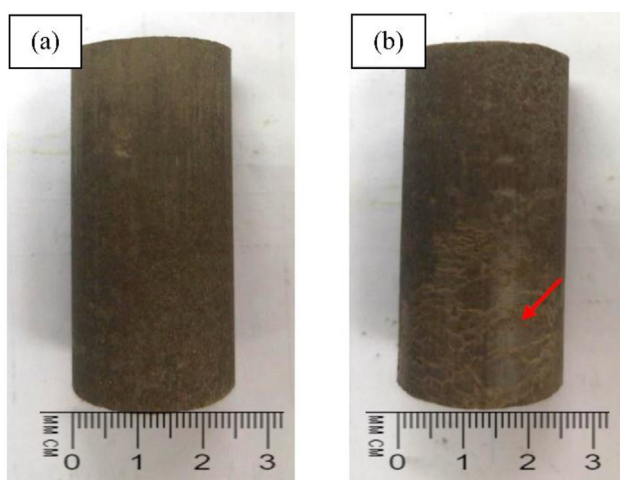


Fig. 12 – Physical observation of geopolymer formed from (a) 3 ton and (b) 6 ton of pressing force.

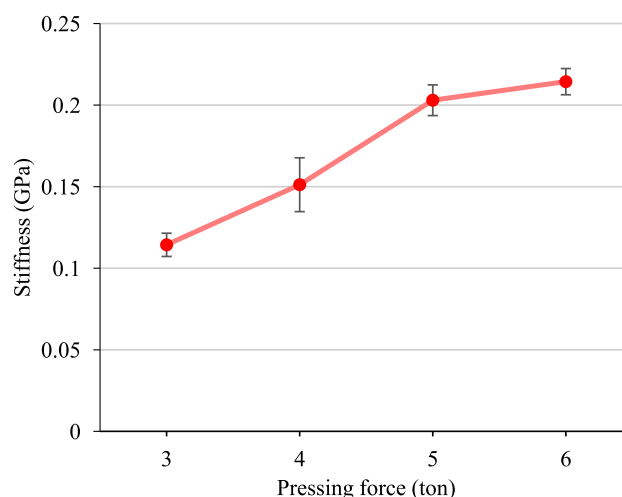


Fig. 13 – The 28-day stiffness of pressed geopolymer with different pressing force.

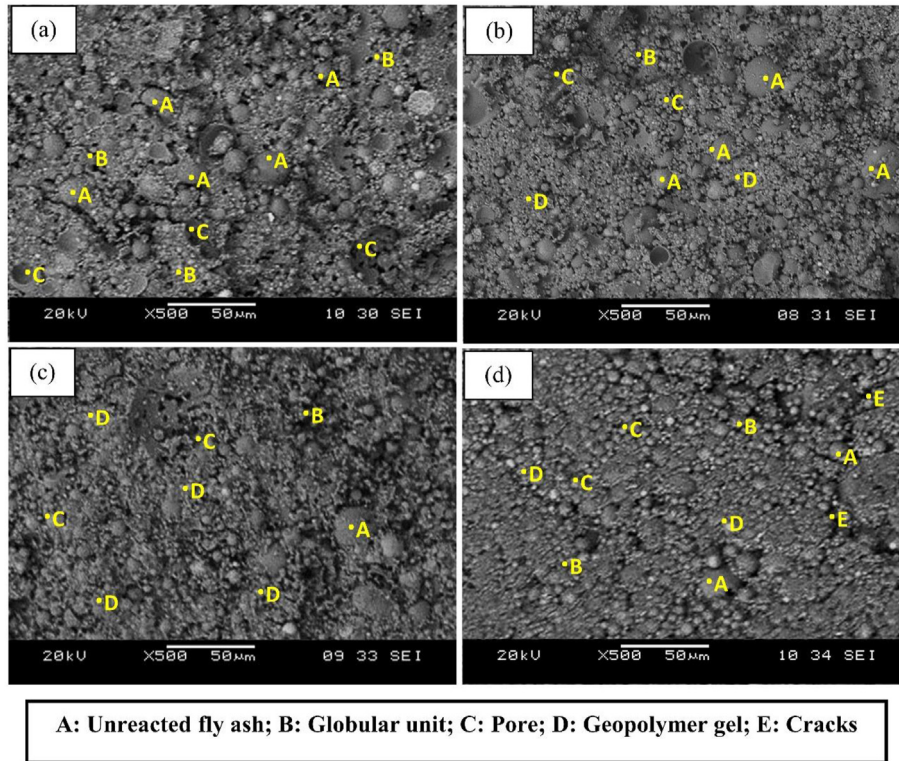


Fig. 14 – SEM micrographs of pressed geopolymers after 28 days with pressing forces of (a) 3 tons; (b) 4 tons; (c) 5 tons; and (d) 6 tons.

the $\text{Al}(\text{OH})_4^-$ species, while the H_2O is combined with the Na_2O through the ion–dipole interaction [35].

The increased $\text{SiO}_2/\text{Na}_2\text{O}$ ratio shifted the chemical reaction towards the generation of silica species and led to the formation of geopolymers with a promising mechanical performance. However, this behaviour is likely to differ depending upon the circumstances. Leong et al. [36] prepared geopolymers with potassium hydroxide (KOH) rather than a NaOH solution improved the geopolymer's compressive strength by reducing the $\text{SiO}_2/\text{Na}_2\text{O}$ ratio. Overall, it is desirable to consider the type of alkali activator used in the fabrication of geopolymers.

In the geopolymer system, H_2O acts as a carrier during the geopolymerisation reaction, which is essential in supporting the hydrolysis reaction of geopolymer binder and improving

the workability of geopolymer mixture. Based on a previous study [35], the initial $\text{H}_2\text{O}/\text{Na}_2\text{O}$ ratio should be between 10.0 and 20.0 to ensure the good workability of the geopolymers for the casting method. This statement was incongruence with the findings of present study since the strength of the pressed geopolymers was degraded when the $\text{H}_2\text{O}/\text{Na}_2\text{O}$ ratio increased to 13.0, which was attributed to the difficulty in the compaction process of the geopolymer mix.

3.6. Effect of pressing force

Table 7 shows the physical properties of the pressed geopolymers obtained using various pressing forces. The density of the pressed geopolymers fell within the range of 2182–2231 kg/m^3 . Generally, the bulk density of fly ash

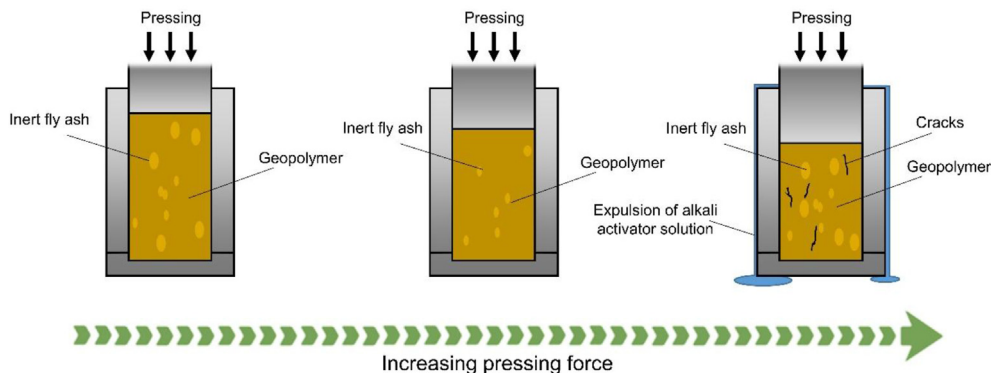


Fig. 15 – Schematic diagram of pressed geopolymer formed by increasing the pressing force.

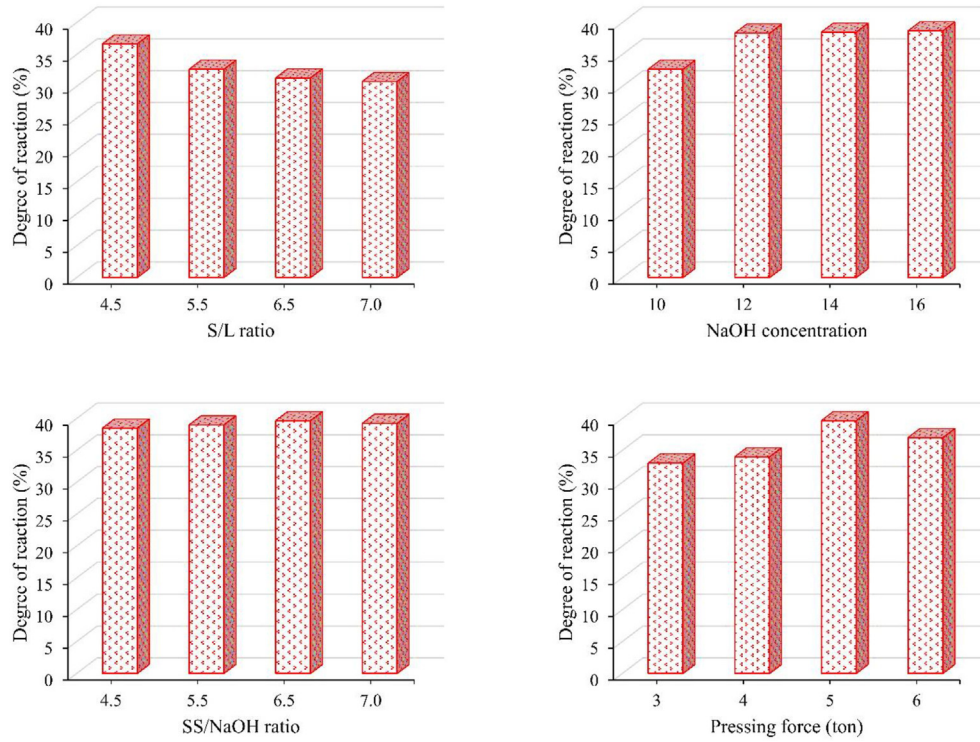


Fig. 16 – Degree of reaction of 28-day pressed geopolymer with different (a) S/L ratio, (b) NaOH concentration, (c) SS/NaOH ratio and (d) pressing force.

geopolymers formed via the casting method lies between 1700 and 1850 kg/m³ [6], while the bulk density of metakaolin geopolymers ranges from 1740 to 1780 kg/m³ [37]. As revealed by the present study, geopolymers formed via the casting

method generally exhibit a comparatively lower density than pressed geopolymers. The increased density of the pressed geopolymers with the increased pressing force was attributed to the inter-particle space and the volume reduction of the geopolymer specimens. Meanwhile, the increased density reduced the porosity and water absorption percentages.

The 7-day and 28-day compressive and flexural strengths of the pressed geopolymer obtained using different pressing

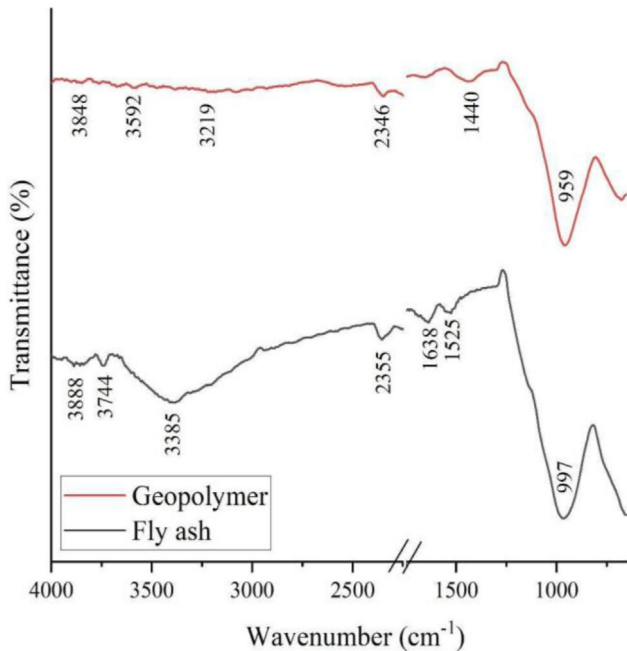


Fig. 17 – FTIR spectra of fly ash and optimized pressed geopolymer.

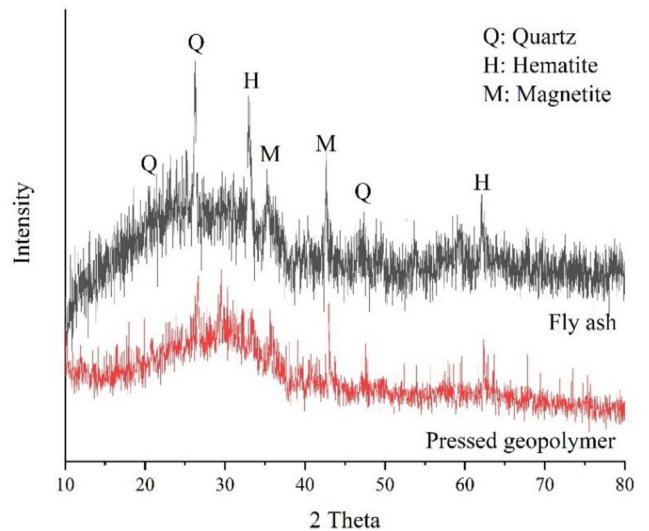


Fig. 18 – XRD patterns of fly ash and optimized pressed geopolymer.

forces are shown in Fig. 11. As the pressing force increases from 3 to 5 tons, the 28-day strength of the pressed geopolymer increased attributed to the structural modification and rearrangement of the geopolymer. This led to a final structure with better strength properties and a lower volume of pores.

However, a further increase in pressing force (>5 tons) had a negative effect on the mechanical properties of the geopolymers. This was related to the fact that when the geopolymer mixture was subjected to 5 tons of pressing force, most of the free pore fractions in the geopolymer matrix disappeared, leaving pore fractions that were confined within the hollow sphere and were difficult to remove [17]. Moreover, the excessive pressing force caused the overflow of the alkali activator, which reduced the degree of geopolymerisation and led to inert fly ash, as confirmed by the inhomogeneous surface (indicated by the red arrow (in the web version) in Fig. 12). The geopolymer sample in Fig. 12a has a smoother and homogeneous surface in which the colour of the sample surface is even. On the other hand, the geopolymer sample that prepared by 6 tons of pressing force (Fig. 12b) has a smooth surface at the top of the sample, but uneven surface at the bottom.

The pressing stress of 100.0 MPa was needed to maximise the compressive strength of geopolymer using the cold-pressing technique is almost four times of that required for the hot-pressing technique (pressing stress of 27.6 MPa) [17].

As Hashimoto et al. [38] proposed, the hot-press treatment has a similar effect as sintering at elevated temperatures, where the removal of the liquid phase and the geopolymerisation tend to be accelerated. In the present study, the specimens were pressed under room temperature conditions, which lowered the degree of reaction between the aluminosilicates and the alkali activator. Therefore, a higher induced stress was required to shorten the space between the solid particles and enhance geopolymerisation.

The stiffness of 28-day pressed geopolymer prepared using different pressing force are shown in Fig. 13. In general, the stiffness of pressed geopolymer increased with pressing force. The increase in pressing force considerably enhanced the structure compactness and reduced the porosity, contributing to the stiffness and flexural strength of geopolymer.

However, the stiffness of geopolymer in present study was considered very low compare to that of other study [39–41]. It was posited that the stiffness of a material was dependent to the stress distributions on the cross-section of material [42]. During the flexural test, the stress will concentrate over a small portion of the material and lead to the distortion of a thin cross-section. Hence, the stiffness of material increased with its thickness. It is foreseeable that the development of stiffness of geopolymer in present study limited due to the low thickness (7 mm) of the samples. In comparison to the hot-pressed geopolymer, the cold-pressed geopolymer presented a lower stiffness despite higher induced stress was used

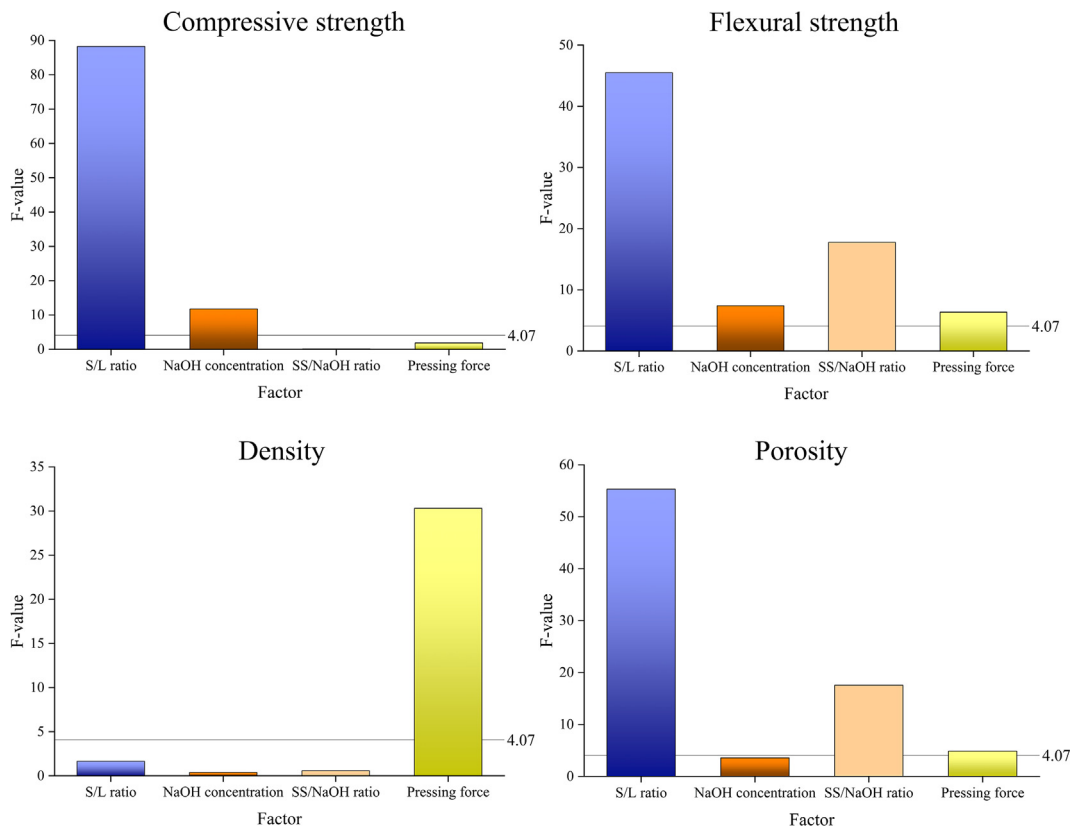


Fig. 19 – F-value in ANOVA analysis for four factors.

during the forming process. The results could be supported by the study of Nasvi et al. [43] which implied that the heat-treated geopolymers are stiffer than the room-cured geopolymer. In light of this, the increased in stiffness with temperature can be explained by the increased in the structural rearrangement and densification of geopolymer which improved the stiffness and brittleness of final product [44].

Fig. 14 depicts SEM images of the pressed geopolymers fabricated using different pressing forces. Fig. 14a (3 tons) and b (4 tons) show identical morphologies, which corresponded to similar compressive strength results (Fig. 11). Both of these geopolymer samples exhibited an inhomogeneous morphology consisting of voids and unreacted fly ash. As noted above, the subjection of a pressing force assists in reducing the inter-particle space of the fly ash, which increases the reactivity of the particles. Thus, it was anticipated that an insufficient pressing force could generate a loosely-packed microstructure, which will, in turn, increase the porosity and water absorption of the pressed geopolymers (Table 7).

The geopolymer subjected to a 5 tons of pressing force indicated a more compact microstructure with less unreacted fly ash particles. However, a further increase in pressing force prompted an increase in the amount of unreacted fly ash corresponding to the overflow of the alkali activator, which hindered the geopolymerisation reaction. As aforementioned, the pressing force induced stress on the geopolymer matrix which lead to the compaction of geopolymer matrix. However, overload of stresses in the samples will be relieved as cracks. Also, the heterogeneous geopolymer materials with geopolymer matrix and unreacted fly ash particles will influence the crack initiation and propagation, depending on the interaction and stresses between the different phases (Fig. 15). The formation of cracks that adversely impacted the mechanical development of the geopolymer.

3.7. Degree of reaction

Fig. 16 shows the degree of reaction of the 28-day pressed geopolymers prepared using different S/L ratios, NaOH concentrations, SS/NaOH ratios and pressing forces. Here, it was clear that the degree of reaction of the pressed geopolymers was inversely proportional to the S/L ratio (Fig. 16a). A lower S/L ratio indicated a higher alkali activator content participating in the geopolymer system, which improved the Si^{4+} and Al^{3+} dissociation and led to a better reaction rate. However, the reactivity of the pressed geopolymers was not necessarily guarantee the greatest mechanical achievement. This was because the comparatively high alkali activator content could destructively affect the development of morphology due to pores formation. The existence of pores will lead to a stress concentration point and result in structural failure. Even when the comparatively higher alkali activator led to greater reactivity; the greater amount of pores substantially reduced the mechanical strength. While the pressed geopolymer with an S/L ratio of 4.5 had the highest degree of reaction, it exhibited the maximum percentage of porosity (Table 4) and the minimum mechanical development (Fig. 4). Another way of saying, while the degree of reaction could be one of the determinants of the strength of pressed geopolymers, the

other design variables will also undoubtedly play a crucial role.

As Fig. 16b shows, the increase in NaOH concentration improved the reaction of the pressed geopolymers due to the dissolution enhancement of the reacting materials. As the SS/NaOH ratio increased from 1.0 to 2.0, the degree of reaction increased from 38.5% to 39.7%. This was due to the increase in the soluble silica content of the sodium silicate, which favoured the polymerisation process of the geopolymerisation and led to the formation of more reaction products. Furthermore, by increasing the pressing force from 3 to 5 tons, the degree of reaction was increased from 33.0% to 39.7%, corresponding to the inter-particle space reduction of fly ash particles, which, as noted above, increases the activity and/or contact between the reacting particles.

3.8. Structural analysis

Fig. 17 manifests the Fourier transform infrared (FTIR) spectra of the fly ash and the optimised pressed geopolymers after 28 days. The FTIR spectrum of the starting fly ash was similar to that of the pressed geopolymers, with the most notable difference between the FTIR spectra associated with the broad band centred at $959\text{--}997\text{ cm}^{-1}$. The main band of fly ash located at 997 cm^{-1} shifted to a lower wavenumber after geopolymerisation. This band was designated as the main band and was attributed to the asymmetric stretching vibration of the Si–O–T bonding, where T is tetrahedral silicon or aluminium [45]. The variation in the position and intensity of the Si–O–T band corresponded to the generation of geopolymeric networks, while the shift also implied a structural organisation where a large number of Al^{3+} ions were incorporated in the SiO_4 tetrahedral with the increase in a non-bridging oxygen structure. This indicated the development of both larger molecular structures and some cross-linking [6].

The bands located at 1638 cm^{-1} corresponded to the bending of chemically bound water, H–O–H, due to the water molecules in the geopolymer framework [46]. The band that appeared at $2346\text{--}2355\text{ cm}^{-1}$ was assigned to the physically bound H–O–H corresponding to the water that was physically absorbed on the surface or trapped in the pores of the geopolymer matrix. Another band resulting from O–H stretching vibration was observed at $3219\text{--}3888\text{ cm}^{-1}$. In addition, the geopolymers underwent atmospheric carbonation, as evidenced by the stretching vibration O–C–O band at $1440\text{--}1525\text{ cm}^{-1}$ [17].

3.9. Phase analysis

Fig. 18 compares the X-ray diffraction (XRD) diffractograms of the fly ash and the optimised pressed geopolymer. The XRD patterns revealed that the fly ash was composed of quartz as the major phase and haematite and magnetite as the minor phases, while the diffuse halo that ranged between 10° and $37^\circ 2\theta$ indicated that the fly ash had a semi-crystalline and amorphous structure.

After the geopolymerisation process, the position of the halo that ranged between 10° and $37^\circ 2\theta$ in the fly ash shifted to higher angular values ($15^\circ\text{--}38^\circ 2\theta$), suggesting the generation of a geopolymeric matrix. According to Criado et al. [47],

quartz presents an unreactive phase. In fact, quartz peaks in the pressed geopolymers indicated that they did not participate in the geopolymerisation process. However, the quartz intensities in the geopolymer were lower than that in the fly ash, attributed to the dilution effect [48]. Based on the XRD patterns, no new crystalline phase was formed.

3.10. Statistical analysis

The F-values obtained via one-way analysis of variance (ANOVA; confidence level = 95%) are shown in Fig. 19. The aim was to investigate the significance of each factor on the compressive strength, flexural strength, density and porosity of the pressed geopolymers. The factors were regarded as insignificant when the statistical F-value was less than the theoretical F-value at a 5% significance level, which was 4.07.

The significant factors that governed the compressive strength development of the pressed geopolymer were the S/L ratio and the NaOH concentration. Here, the S/L ratio had the greatest impact on the compressive strength among all the factors. In terms of the F-value of the flexural strength of the pressed geopolymers, all the factors (S/L ratio, NaOH concentration, SS/NaOH ratio and pressing force) were significant in the following sequence: S/L ratio > SS/NaOH ratio > NaOH concentration > pressing force. The S/L ratio had the most influence on the strength development since it ensured the feasibility of producing the specimen and the acceptable content of alkali activator for the progress of the geopolymerisation reaction.

Besides, the density of the pressed geopolymer was only affected by the pressing force used during the compaction process. The force significantly reduced the pores and enhanced the compactness of the geopolymers. The S/L ratio and the SS/NaOH ratio were the decisive factors in the porosity of the pressed geopolymers, given that these ratios determined the amount of liquid medium in the geopolymer mixture. When the liquid medium was high, the corresponding porosity was also high.

In partial sum, except for the density of the pressed geopolymers, the S/L ratio had the most significant impact on the properties of the pressed geopolymers. This ratio influenced the pressing characteristics of the geopolymers and changed the morphology of the resultant products.

4. Conclusion

In this paper, various experimental investigations determined the effects of S/L ratio, NaOH concentration, SS/NaOH ratio and pressing force on the physical and mechanical properties of pressed geopolymers as well as their reactivity. The optimal pressed geopolymer was formed using S/L ratio of 5.5, NaOH concentration of 14 M, SS/NaOH ratio of 2.0 and pressing force of 5 tons. The resultant pressed geopolymer achieved excellent 28-day compressive and flexural strengths of 114.2 and 29.9 MPa, respectively. With a lower alkali activator content, the compressive strength of the cold-pressed geopolymers was comparable to that of hot-pressed geopolymers. A longer ageing time is required for the former.

Based on the results obtained from the one-way ANOVA analysis, the S/L ratio had the most significant effect on the compressive strength, flexural strength and porosity of the pressed geopolymers. Their density was only influenced by the pressing force used in the compaction process. Hence, compared to the casting method, the presence of a pressing force and a lower S/L offers the possibility of developing better physical and mechanical properties of geopolymers. The high compressive and flexural strength achieved in this work validated the potential of cold-pressed geopolymers for application as functional building materials such as precast concrete and tiles.

Declaration of Competing Interest

The authors declare that they have no known competing financial interests or personal relationships that could have appeared to influence the work reported in this paper.

Acknowledgement

The authors gratefully acknowledge the support by Fundamental Research Grant Scheme (FRGS/1/2020/TK0/UNIMAP/02/42) from the Ministry of Higher Education, Malaysia.

REFERENCES

- [1] Damtoft JS, Lukasik J, Herfort D, Sorrentino D, Gartner EM. Sustainable development and climate change initiatives. *Cem Concr Res* 2008;38:115–27. <https://doi.org/10.1016/j.cemconres.2007.09.008>.
- [2] Song H, Wei L, Ji Y, Cao L, Cheng F. Heavy metal fixing and heat resistance abilities of coal fly ash-waste glass based geopolymers by hydrothermal hot pressing. *Adv Powder Technol* 2018;29:1487–92. <https://doi.org/10.1016/j.apt.2018.03.013>.
- [3] Guo X, Yang J, Xiong G. Influence of supplementary cementitious materials on rheological properties of 3D printed fly ash based geopolymer. *Cem Concr Compos* 2020;114:103820. <https://doi.org/10.1016/j.cemconcomp.2020.103820>.
- [4] Ye J, Zhang W, Shi D. Properties of an aged geopolymer synthesized from calcined ore-dressing tailing of bauxite and slag. *Cem Concr Res* 2017;100:23–31. <https://doi.org/10.1016/j.cemconres.2017.05.017>.
- [5] Albidah A, Abadel A, Alrshoudi F, Altheeb A, Abbas H, Al-Salloum Y. Bond strength between concrete substrate and metakaolin geopolymer repair mortars at ambient and elevated temperatures. *J Mater Res Technol* 2020;9:10732–45. <https://doi.org/10.1016/j.jmrt.2020.07.092>.
- [6] Zhang M, Zhao M, Zhang G, Sietins JM, Granados-Focil S, Pepi MS, et al. Reaction kinetics of red mud-fly ash based geopolymers: effects of curing temperature on chemical bonding, porosity, and mechanical strength. *Cem Concr Compos* 2018;93:175–85. <https://doi.org/10.1016/j.cemconcomp.2018.07.008>.
- [7] Ke S, Wang Y, Pan Z, Ning C, Zheng S. Recycling of polished tile waste as a main raw material in porcelain tiles. *J Clean Prod* 2016;115:238–44. <https://doi.org/10.1016/j.jclepro.2015.12.064>.

- [8] Wang H, Zhu M, Sun Y, Ji R, Liu L, Wang X. Synthesis of a ceramic tile base based on high-alumina fly ash. *Constr Build Mater* 2017;155:930–8. <https://doi.org/10.1016/j.conbuildmat.2017.07.049>.
- [9] Andreola F, Barbieri L, Queiroz Soares B, Karamanov A, Schabbach LM, Bernardin AM, et al. Toxicological analysis of ceramic building materials – tiles and glasses – obtained from post-treated bottom ashes. *Waste Manag* 2019;98:50–7. <https://doi.org/10.1016/j.wasman.2019.08.008>.
- [10] Prasanphan S, Wannagon A, Kobayashi T, Jiemsirilers S. Reaction mechanisms of calcined kaolin processing waste-based geopolymers in the presence of low alkali activator solution. *Constr Build Mater* 2019;221:409–20. <https://doi.org/10.1016/j.conbuildmat.2019.06.116>.
- [11] Wang S, Ma X, He L, Zhang Z, Li L, Li Y. High strength inorganic-organic polymer composites (IOPC) manufactured by mold pressing of geopolymers. *Constr Build Mater* 2019;198:501–11. <https://doi.org/10.1016/j.conbuildmat.2018.11.281>.
- [12] Khater HM, Ezzat M. Preparation and characterization of engineered stones based geopolymer composites. *J Build Eng* 2018;20:493–500. <https://doi.org/10.1016/j.jobe.2018.08.004>.
- [13] Alshaaer M. Two-phase geopolymerization of kaolinite-based geopolymers. *Appl Clay Sci* 2013;86:162–8. <https://doi.org/10.1016/j.clay.2013.10.004>.
- [14] Wang H, Li H, Yan F. Synthesis and mechanical properties of metakaolinite-based geopolymer. *Colloids Surf A Physicochem Eng Asp* 2005;268:1–6. <https://doi.org/10.1016/j.colsurfa.2005.01.016>.
- [15] Takeda H, Hashimoto S, Matsui H, Honda S, Iwamoto Y. Rapid fabrication of highly dense geopolymers using a warm press method and their ability to absorb neutron irradiation. *Constr Build Mater* 2014;50:82–6. <https://doi.org/10.1016/j.conbuildmat.2013.09.014>.
- [16] Carter CB, Norton MG. *Ceramic materials: science and engineering*. New York: Springer; 2013. https://books.google.com.my/books?id=WRg_AAAAQBAJ.
- [17] Ranjbar N, Mehrali M, Maheri MR, Mehrali M. Hot-pressed geopolymer. *Cem Concr Res* 2017;100:14–22. <https://doi.org/10.1016/j.cemconres.2017.05.010>.
- [18] Posi P, Thongjapo P, Thamultree N, Boontee P, Kasemsiri P, Chindaprasirt P. Pressed lightweight fly ash-OPC geopolymer concrete containing recycled lightweight concrete aggregate. *Constr Build Mater* 2016;127:450–6. <https://doi.org/10.1016/j.conbuildmat.2016.09.105>.
- [19] Chindaprasirt P, Thaiwitcharoen S, Kaewpirom S, Rattanasak U. Controlling ettringite formation in FBC fly ash geopolymer concrete. *Cem Concr Compos* 2013;41:24–8. <https://doi.org/10.1016/j.cemconcomp.2013.04.009>.
- [20] Hao H, Lin K, Wang D, Chao S, Shiu H, Si A. Utilization of solar panel waste glass for metakaolinite-based geopolymer synthesis. *Environ Prog Sustain Energy* 2013;32:797–803. <https://doi.org/10.1002/ep>.
- [21] Capes CE. *Particle size Enlargement*. 1st ed. Elsevier; 1980.
- [22] Saha S, Rajasekaran C. Enhancement of the properties of fly ash based geopolymer paste by incorporating ground granulated blast furnace slag. *Constr Build Mater* 2017;146:615–20. <https://doi.org/10.1016/j.conbuildmat.2017.04.139>.
- [23] Zhao M, Zhang G, Htet KW, Kwon M, Liu C, Xu Y, et al. Freeze-thaw durability of red mud slurry-class F fly ash-based geopolymer: effect of curing conditions. *Constr Build Mater* 2019;215:381–90. <https://doi.org/10.1016/j.conbuildmat.2019.04.235>.
- [24] Tan J, Lu W, Huang Y, Wei S, Xuan X, Liu L, et al. Preliminary study on compatibility of metakaolin-based geopolymer paste with plant fibers. *Constr Build Mater* 2019;225:772–5. <https://doi.org/10.1016/j.conbuildmat.2019.07.142>.
- [25] Astutiningsih S, Tambun D, Zakiyuddin A. Characterization and comparison of geopolymer synthesized using metakaolin Bangka and Metastar as precursors. *E3S Web Conf* 2018;67:1–6. <https://doi.org/10.1051/e3sconf/20186703022>.
- [26] Nazari A, Sanjayan JG. Synthesis of geopolymer from industrial wastes. *J Clean Prod* 2015;99:297–304. <https://doi.org/10.1016/j.jclepro.2015.03.003>.
- [27] Livi CN, Repette WL. Effect of NaOH concentration and curing regimes on compressive strength of fly ash-based geopolymer. *Rev IBRACON Estruturas e Mater* 2017;10:1174–81. <https://doi.org/10.1590/S1983-41952017000600003>.
- [28] Posi P, Teerachanwit C, Tanutong C, Limkamoltip S, Lertnimooolchai S, Sata V, et al. Lightweight geopolymer concrete containing aggregate from recycle lightweight block. *Mater Des* 2013;52:580–6. <https://doi.org/10.1016/j.matdes.2013.06.001>.
- [29] Hadi MNS, Zhang H, Parkinson S. Optimum mix design of geopolymer pastes and concretes cured in ambient condition based on compressive strength, setting time and workability. *J Build Eng* 2019;23:301–13. <https://doi.org/10.1016/j.jobe.2019.02.006>.
- [30] Bahador Moradikhrou A, Esparham A. Factors influencing compressive strength of metakaolin-based geopolymer concrete. *Modares Civ Eng J* 2020;20:53–66. <https://mcej.modares.ac.ir/article-16-34347-en.html>. [Accessed 6 May 2021].
- [31] Koushkbaghi M, Alipour P, Tahmouresi B, Mohseni E, Saradar A, Sarker PK. Influence of different monomer ratios and recycled concrete aggregate on mechanical properties and durability of geopolymer concretes. *Constr Build Mater* 2019;205:519–28. <https://doi.org/10.1016/j.conbuildmat.2019.01.174>.
- [32] Haddad RH, Alshbuol O. Production of geopolymer concrete using natural pozzolan: a parametric study. *Constr Build Mater* 2016;114:699–707. <https://doi.org/10.1016/j.conbuildmat.2016.04.011>.
- [33] Almalkawi AT, Balchandra A, Soroushian P. Potential of using industrial wastes for production of geopolymer binder as green construction materials. *Constr Build Mater* 2019;220:516–24. <https://doi.org/10.1016/j.conbuildmat.2019.06.054>.
- [34] Mohseni E. Assessment of Na₂SiO₃ to NaOH ratio impact on the performance of polypropylene fiber-reinforced geopolymer composites. *Constr Build Mater* 2018;186:904–11. <https://doi.org/10.1016/j.conbuildmat.2018.08.032>.
- [35] Juengsuwattananon K, Winnefeld F, Chindaprasirt P, Pimraksa K. Correlation between initial SiO₂/Al₂O₃, Na₂O/Al₂O₃, Na₂O/SiO₂ and H₂O/Na₂O ratios on phase and microstructure of reaction products of metakaolin-rice husk ash geopolymer. *Constr Build Mater* 2019;226:406–17. <https://doi.org/10.1016/j.conbuildmat.2019.07.146>.
- [36] Leong HY, Ong DEL, Sanjayan JG, Nazari A. The effect of different Na₂O and K₂O ratios of alkali activator on compressive strength of fly ash based-geopolymer. *Constr Build Mater* 2016;106:500–11. <https://doi.org/10.1016/j.conbuildmat.2015.12.141>.
- [37] Liang G, Zhu H, Zhang Z, Wu Q, Du J. Investigation of the waterproof property of alkali-activated metakaolin geopolymer added with rice husk ash. *J Clean Prod* 2019;230:603–12. <https://doi.org/10.1016/j.jclepro.2019.05.111>.
- [38] Hashimoto S, Shimoda W, Takeda H, Daiko Y, Honda S, Iwamoto Y. Fabrication of slaked lime compacts (plasters) with high compressive strength using a warm press method. *Constr Build Mater* 2016;110:65–9. <https://doi.org/10.1016/j.conbuildmat.2016.02.009>.

- [39] Daniel AJ, Sivakamasundari S, Abhilash D. Comparative study on the behaviour of geopolymer concrete with hybrid fibers under static cyclic loading. *Procedia Eng* 2017;173:417–23. <https://doi.org/10.1016/j.proeng.2016.12.041>.
- [40] Singh S, Aswath MU, Ranganath RV. Performance assessment of red mud based geopolymer bricks and prisms. *J Build Eng* 2020:101462. <https://doi.org/10.1016/j.jobe.2020.101462>.
- [41] Kalaivani M, Shyamala G, Ramesh S, Angusenthil K, Jagadeesan R. Performance evaluation of fly ash/slag based geopolymer concrete beams with addition of lime. *Mater Today Proc* 2020:1–5. <https://doi.org/10.1016/j.matpr.2020.01.596>.
- [42] Patton R, Li F, Edwards M. Causes of weight reduction effects of material substitution on constant stiffness components. *Thin Walled Struct* 2004;42:613–37. <https://doi.org/10.1016/j.tws.2003.08.001>.
- [43] Nasvi MM, Gamage RP, Jay S. Geopolymer as well cement and the variation of its mechanical behavior with curing temperature. *Greenh Gases Sci Technol* 2012;2:46–58. <https://doi.org/10.1002/ghg>.
- [44] Bernal SA, Bejarano J, Garzón C, de Gutiérrez RM, Delvasto S, Rodríguez ED. Performance of refractory aluminosilicate particle/fiber-reinforced geopolymer composites. *Compos B Eng* 2012;43:1919–28. <https://doi.org/10.1016/j.compositesb.2012.02.027>.
- [45] Xue X, Liu YL, Dai JG, Poon CS, Zhang WD, Zhang P. Inhibiting efflorescence formation on fly ash-based geopolymer via silane surface modification. *Cem Concr Compos* 2018;94:43–52. <https://doi.org/10.1016/j.cemconcomp.2018.08.013>.
- [46] Almalkawi AT, Balchandra A, Soroushian P. Potential of using industrial wastes for production of geopolymer binder as green construction materials. *Constr Build Mater* 2019;220:516–24. <https://doi.org/10.1016/j.conbuildmat.2019.06.054>.
- [47] Criado M, Fernández-Jiménez A, de la Torre AG, Aranda MAG, Palomo A. An XRD study of the effect of the $\text{SiO}_2/\text{Na}_2\text{O}$ ratio on the alkali activation of fly ash. *Cem Concr Res* 2007;37:671–9. <https://doi.org/10.1016/j.cemconres.2007.01.013>.
- [48] Heah CY, Kamarudin H, Mustafa Al Bakri AM, Bnhussain M, Luqman M, Khairul Nizar I, et al. Study on solids-to-liquid and alkaline activator ratios on kaolin-based geopolymers. *Constr Build Mater* 2012;35:912–22. <https://doi.org/10.1016/j.conbuildmat.2012.04.102>.